

Gravitational Microlensing by Rotating Stars

Habib Ebrahimnejad Rahbari¹, Mohammad Nouri-Zonoz^{1,3} and Sohrab Rahvar^{2,3}

nouri@khayam.ut.ac.ir

rahvar@sharif.edu

ABSTRACT

Using astrometry of microlensing events we study the effect of angular momentum as compared to that of the parallax. For a rotating lens it is shown that the effect of the angular momentum deviates the center of images from that in the simple standard microlensing. This effect could be observed by future astrometry missions such as GAIA and SIM for lenses with angular momentum $S \gtrsim \times 10^{48} \text{kgm}^2 \text{sec}^{-1}$. It is shown that for extreme black hole lenses the corresponding mass should be more than $10^3 M_{\odot}$.

Subject headings: gravitation – stars: rotation – cosmology: gravitational lensing

1. Introduction

Gravitational lensing and microlensing have been treated and employed as powerful tools to study astrophysical objects and phenomena (Schneider, Ehlers and Falco 1993; Mollerach, Esteban 2002). Among many examples and applications one could mention the search for MACHO candidates at the galactic halo using gravitational microlensing with the recent data pointing at the absence of them (Tisserand and Milsztajn 2005). Other application of gravitational microlensing include (a) study of stellar atmosphere (Cassan et al. 2004; Abe et al. 2003; Bryce et al. 2002), (b) planet searching (Bennet et al. 1999), (c) exotic matter searches such as magnetic masses (Rahvar & Nouri-Zonoz 2003; Nouri-Zonoz and Lynden-Bell 1997; Lynden-Bell and Nouri-Zonoz 1998) and wormholes (Safonova, Torres and Romero 2002), (d) possible black hole detection based on gravitational microlensing method (Agol et. al

¹Department of Physics, University of Tehran, North Karegar St., Tehran 14395-547, Iran

²Department of Physics, Sharif University of Technology, P.O.Box 11365-9161, Tehran, Iran

³Institute for Studies in Theoretical Physics and Mathematics, P.O.Box 19395-5531, Tehran, Iran

2002). Furthermore it seems that future observations will be based on astrometric microlensing which is hoped to improve previous studies. Another application which is the concern of this paper includes angular momentum detection by photometric and astrometric microlensing. This in turn could enhance detection of black hole candidates through this extra parameter.

The outline of the paper is as follows: In Section 2 we introduce photometric and astrometric microlensing. Section 3 contains gravitational microlensing in kerr metric and sensitivity of angular momentum detection to the lens parameters. Conclusion and summery are given in Section 4.

2. Photometric and Astrometric Microlensing

Simple microlensing events occur when the approximation of a point-like deflector and point-like source in a relative uniform motion is valid in the Galactic scale (Paczynski 1986). At a given time t , the light magnification $A(t)$ of a point-like source located at lens-source D_{ls} and observer-lens D_{ol} distances induced by a point-like deflector of mass M is given by:

$$A(t) = \frac{u^2(t) + 2}{u(t)\sqrt{4 + u^2(t)}}, \quad (1)$$

where $u(t)$ is the impact parameter (distance between lens and source in the lens plane), expressed in units of the "Einstein Radius" R_E and is given by:

$$R_E = \sqrt{\frac{4GDM}{c^2}} \quad , \quad D = \frac{D_{ol}D_{ls}}{D_{os}}, \quad (2)$$

where G is the Newtonian gravitational constant and c is the velocity of light. Assuming a source moving at a constant relative transverse speed v_T , reaching its minimum distance u_0 to the lens in the lens plane at time t_0 , $u(t)$ is given by:

$$u(t) = \sqrt{u_0^2 + \left(\frac{t - t_0}{t_E}\right)^2} \quad , \quad t_E = \frac{R_E}{v_T}, \quad (3)$$

where t_E , the "Einstein crossing time", is the only measurable parameter providing useful information about the lens in the approximation of the simple microlensing. Within this approximation, the light-curve of a microlensed star is fully determined by the parameters F_b, u_0, t_0 and t_E . In the next two subsections we introduce astrometry and parallax effect and their signature in the gravitational microlensing.

2.1. Astrometric microlensing in Schwarzschild space time

For a point like source at distance $u = \frac{b}{R_E}$ in the lens plane from a point like gravitational lens, it is well known that the images are located at:

$$u_{\pm}^I = \frac{u \pm \sqrt{u^2 + 4}}{2}. \quad (4)$$

Corresponding amplifications are given by:

$$A_{\pm} = \frac{1}{2} \left(1 \pm \frac{2 + u^2}{u \sqrt{u^2 + 4}} \right). \quad (5)$$

The location of the center of images with respect to lens, in the lens plane, is defined by:

$$\mathbf{R}_{image} = \frac{\mathbf{u}_+^I |A_+| + \mathbf{u}_-^I |A_-|}{|A_+| + |A_-|}. \quad (6)$$

We are interested in the deflection of the combined images, i.e. the location of centroid with respect to the source, so we transform \mathbf{R}_{image} to \mathbf{R}'_{image} i.e :

$$\mathbf{R}'_{image} = \mathbf{R}_{image} - \mathbf{u} \quad \text{then} \quad \mathbf{R}'_{image} = \frac{u}{u^2 + 2} \frac{\mathbf{u}}{u}. \quad (7)$$

As u changes with time \mathbf{R}'_{image} plots a pattern. In the case of the Schwarzschild space-time the pattern is an ellipse.

To study the asymptotic behavior of the standard astrometric microlensing, we examine equation (7). If $u \rightarrow \infty$, the centroid shift falls off like $\frac{1}{u}$, this can be compared with the photometric amplification A , which falls off like: $\frac{1}{u^2}$. These asymptotic results illustrate one of the important differences between astrometric and photometric microlensing namely that the *centroid shift falls off much more slowly than amplification*. In consequence, cross section for astrometric events is much larger than that for photometric events (Miralda-Escude 1996; Dominik & Sahu 2000; Honma 2001).

2.2. Parallax effect in microlensing

If the variation of the Earth's velocity around the sun is not negligible with respect to the projected transverse speed of the deflector, then the apparent trajectory of the deflector with respect to the line of sight is a cycloid instead of a straight line. The resulting amplification versus time is therefore affected by the so-called *parallax effect*. This effect is more easily observable for long duration events (several months), for which the change in the Earth's velocity is important (Alcock et al. 1995). If $\mathbf{u}_D(t)$ is the position of the deflector in the

deflector’s transverse plane and $\mathbf{u}_E(t)$ is the intercept of the Earth-source line of sight with this plane, then:

$$u(t) = |\mathbf{u}_D(t) - \mathbf{u}_E(t)|^{\frac{1}{2}}, \quad (8)$$

where

$$\mathbf{u}_D(t) = \left(\frac{t-t_0}{t_E} \cos\theta - u_0 \sin\theta\right) \hat{\mathbf{i}} + \left(\frac{t-t_0}{t_E} \sin\theta - u_0 \cos\theta\right) \hat{\mathbf{j}}, \quad (9)$$

and θ is the angle between the projected lens trajectory and the projected major axis of the Earth’s orbit in the deflector plane. Here u_0 is the closest approach of the lens to the sun at the lens plane. Neglecting the Earth’s orbital eccentricity, $\mathbf{u}_E(t)$ is given by:

$$\mathbf{u}_E(t) = \delta u \sin(\xi(t)) \hat{\mathbf{i}} - \delta u \cos(\xi(t)) \cos(\beta) \hat{\mathbf{j}}, \quad (10)$$

where $\delta u = a_{\oplus}(1-x)/R_E$ is the projection of the Earth’s orbital radius in the deflector plane in unit of Einstein radius and $x = \frac{D_{ol}}{D_{os}}$, β is the angle between the ecliptic and deflector planes and $\xi(t)$ is the phase of the Earth relative to its position at $\mathbf{u}_E = \delta u \cos(\beta) \hat{\mathbf{j}}$. The distortion of the light curve is important if the Earth’s orbital velocity around the sun is not negligible with respect to the projected transverse speed of the deflector:

$$\tilde{v} = \frac{R_E}{t_E(1-x)} = \frac{a_{\oplus}}{\delta u t_E} \quad (11)$$

Rahvar et al. (2003) proposed an observation strategy, using the alert and follow-up telescopes for that can put constrain on the mass and distance of lens in the direction of Magellanic Clouds. Adding a third telescope such as GAIA or SIM one can break the degeneracy between the parameters of lens through astrometric measurements (Rahvar and Ghassemi 2005). Fig. 1 shows the photometry and the astrometry of center of images for the case of simple and considering the parallax effects for a typical lens located at $5kpc$ from the observer with the source star at $10kpc$.

3. Microlensing in Kerr space

Gravitational lensing in the field of a rotating star has been studied previously, for example in (Bray 1986; Ibanez 1983; Glicenstein 1999). Here we employ the formalism introduced by Ibanez (1983) in which the first approximation in G of Kerr metric was used. In the slow-motion or the fast-motion approximation, the bending angle is given by:

$$\Delta \mathbf{n} = -\frac{2}{c} \int_{-\infty}^{+\infty} \nabla \phi dt + \frac{4G}{c^3 b^2} \left[\frac{2}{b^2} \mathbf{b} \cdot (\mathbf{n}_i \times \mathbf{S}) \mathbf{b} - (\mathbf{n}_i \times \mathbf{S}) \right], \quad (12)$$

where \mathbf{b} is the impact parameter, \mathbf{S} spin of the lens and \mathbf{n}_i a unit vector representing the initial direction of incoming photons toward the lens. We note that for \mathbf{S} normal to the

lens plane, the second term in the right hand side of equation (12) vanishes and we can not observe the signature of angular momentum on the position of images. The relation between the position of image and source at the lens plane perpendicular to the line of sight is given by:

$$x_0 = x + \frac{R_E^2}{x_0^2 + y_0^2}x_0 + \frac{2R^2}{(x_0^2 + y_0^2)^2}x_0^2 - \frac{R^2}{x_0^2 + y_0^2}. \quad (13)$$

$$y_0 = y + \frac{R_E^2}{x_0^2 + y_0^2}y_0 + \frac{2R^2}{(x_0^2 + y_0^2)^2}x_0y_0, \quad (14)$$

where $R^2 = \frac{4GSD}{c^3}$ and S is the projected angular momentum on the lens plane. (x, y) and (x_0, y_0) are the components of the source and image positions respectively. (Y-axis is chosen along projection of spin at the lens plane). At the lens plane, the ratio of the terms corresponding to that of the angular momentum to the of mass, in the deviation of light ray is $R^2/R_E^2x_0 = S/c/Mx_0 = (v/c)(R_g/x_0)$, where v is the rotation speed of lens, R_g is gyration radius and x_0 is the position of images. Since $v \ll c$ and $R_g \ll x_0$, the ratio of the spin to the mass term should be smaller than one, means that $S \ll Mx_0c$. For a typical lens of solar mass, in the Milky Way, the images are produced at an astronomical distance from the lens, in other words $S \ll 10^{50}kgm^2/sec$. For lenses with larger masses and located at the galactic scale, the upper limit on the spin will be higher.

For a given source, equations (13) and (14) in principle have three solutions, which means that rotating stars produce three images through lensing where the third image is very close to the lens. Glicenstein (1999) has showed that the third image having a very small impact parameter, it always eclipsed by the lens itself. Using equations (13) and (14), the amplification of the light of an image produced by a rotating lens is given by:

$$A = \left(1 - \frac{R_E^4}{b^4} - \frac{4R^4}{b^6} - \frac{4R^2R_E^2x_0}{b^6}\right)^{-1} \quad (15)$$

3.1. Astrometric microlensing in Kerr space

As the equations (13) and (14) are too complex to be solved analytically, we employ the method of initial guess and substitute the schwarzschild solution in (13) and (14) and through iteration obtain the location of images in the linear Kerr metric. Fig. 2 shows the astrometry of the center of images and the photometry of a microlensing event by a rotating star. Similar to the case of Schwarzschild metric the parallax effect alters the path of center of images in the Kerr metric. Astrometries in Schwarzschild and Kerr metrics with and without the parallax effect are compared in Fig. 3. Since the parallax is not an intrinsic

effect it alters the center of images with the same amount both in Kerr and Schwarzschild spaces, Fig .3. Subtraction of the parallax effect from the path of the center of the images may help us to distinguish the Kerr from Schwarzschild metric.

In practice, the astrometric measurements can be done by a ground-based telescope accompanying a space-based interferometry telescope. The ground-based telescope signals the microlensing events and undertakes photometric measurement and the space-based telescope measures the displacement of image centroids. We examine the sensitivity of angular momentum detection as a function of lens parameters. To do so we need a Monte Carlo simulation generating the mass function as well as the corresponding angular momentum for a given direction of Milky Way and use observational efficiency to estimate the number of events. However, since the dependence of angular momentum to the mass function of stars is not well know, we generate a uniform distribution of lens parameters and use the criterion that the difference between the astrometry of Kerr and ordinary lenses should be more than the angular resolution of GAIA or SIM ($10\mu as >$). The fraction of events with the detectable angular momentum is shown in Fig. 4. It is seen that the angular momentum detection is correlated to all of the parameters of the lens. Increasing the spin, in contrast to the mass rises the detection probability. Very short and long Einstein crossing times are not favored for the spin detection but on the other hand small impact parameter is more convenient for our propose. The distance of lens from the observer also decreases the sensibility of angular momentum detection. The effect of distance decreases the displacement of center of images, Fig. 4.

4. Conclusion

In the present study we examined the possibility of angular momentum detection of rotating lenses by the gravitational microlensing. Out of two methods of photometric and astrometric microlensing, the latter is more feasible. Future space-based interferometry telescopes such as GAIA and SIM can be used for this purpose. Studying the detection sensitivity in terms of the lens parameters showed that the centriod of images in the lenses with angular momentum larger than $S \gtrsim \times 10^{48} kgm^2 sec^{-1}$ deviates more than $10\mu a$ from that of the Schwarzschild case. Recent analysis of X-ray spectral data from *ASCA* and *RXTE* of the two black hole candidates GRO J1655-40 and 4U 1543-47 has estimated the corresponding dimensionless spin parameter $a_* = (Sc/GM^2)$, $\sim 0.7 - 0.75$ and $\sim 0.85 - 0.9$ respectively (Shafee et al. 2005). Considering our estimation of the spin detection limit implies that the mass of an extreme black hole ($a_* = 1$) with observable angular momentum should be more than $10^3 M_\odot$.

Acknowledgments

The authors would like to thank S.E. Vazquez, O. Wucknitz, L. Wisotzki and C. Fendt for their useful comments and for providing some of the references. M-NZ and H.E also thank University of Tehran for supporting this project under the grants provided by the research council.

REFERENCES

- Abe, F. et al., 2003, A&A, 411, 493
- Agol, E., Kamionkowski, M., Koopmans, L. V. E., Blandford, R. D., 2002, ApJ, 576, 131
- Alcock, C., Allsman, R. A., Alves D., et al., 1995, ApJ, 454, L125
- Bennett D. P. et al., 1999, Nature, 402, 57
- Bray, I., 1986, Phys. Rev. D., 34, 367
- Bryce, H. M., Hendry, M. A.m Valls-Gabaud, D., 2002, A&A, 388, 1
- Cassan, A. et al., 2004, A&A, 419, 1
- Dominik, M., Sahu, K. C., 2000, ApJ, 534, 213
- Glicenstein, J. F., 1999, A&A, 343, 1025
- Honma, M., 2001, PASJ, 53, 233
- Ibanez, J., 1983, A&A, 124, 175
- Lynden-Bell D., Nouri-Zonoz M., Rev. Mod. Phys. 70,427, (1998).
- Miralda-Escude, J., 1996, ApJ, 470, L113
- Mollerach, S., Roulet, E., Gravitational Lensing and Microlensing, World Scientific Publisher, 2002
- Nouri-Zonoz M., Lynden-Bell D., 1997, MNRAS, 292, 714
- Paczynski B., 1986, APJ 304, 1.
- Rahvar, S., Nouri-Zonoz, M., 2003, MNRAS, 338, 926

Rahvar, S., Moniez, M., Ansari, R. and Perdereau, O., 2003, A&A, 412, 81

Rahvar, S., Ghassemi S., 2005, A&A, 438, 153

Safonova, M., Torres, D. F. and Romero, G. E., 2002, Phys. Rev. D, 65, 3001

Schneider, P., Ehlers, J. and Falco, E. E., Gravitational Lenses, Springer Verlag, 1993.

Shafee, R., McClintock J. E., Narayan, R., Davis Sh. W., Li, L. and Remillard R. A.,
Submitted to ApJ Letters (astro-ph/0508302).

Tisserand P., Milsztajn A., 2005, To appear in the proceedings of the 5th Rencontres du
Vietnam, "New Views on the Universe" (astro-ph/0501584)

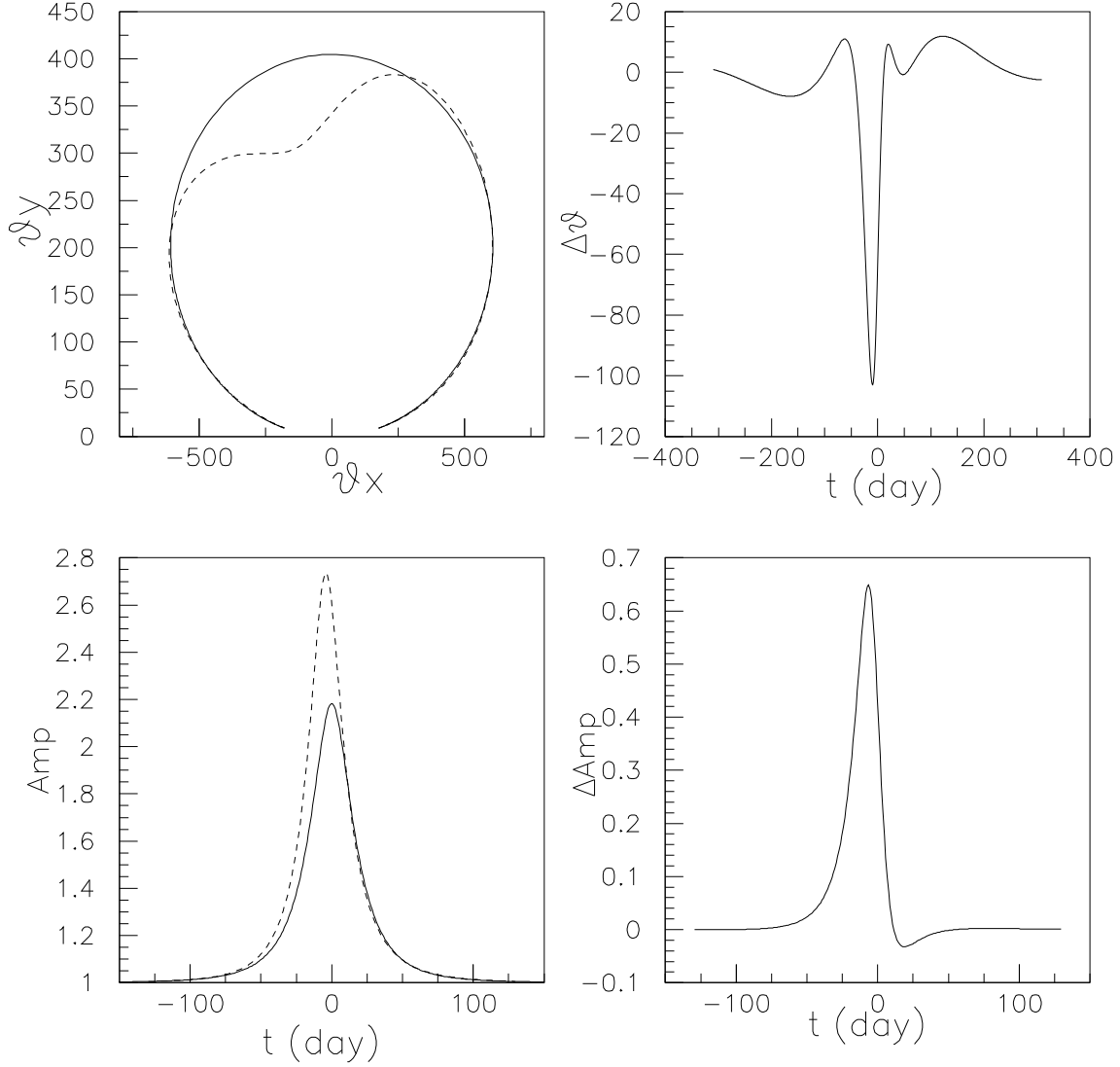


Fig. 1.— Astrometry and Photometry of a microlensing event in schwarzschild metric. The simple microlensing event (solid-line) is compared with considering the parallax effect (dashed-line). Top-left panel shows the astrometry of center of images for both cases and at top-right panel the contrast between them is shown. The lower-left panel is the photometry and the lower-right panel is the contrast between them. The parameters of lens is chosen as $t_e = 40$ days, $t_0 = 0$, $u_0 = 0.5$, $M = M_\odot$, $D_{os} = 10kpc$ and $D_{ls} = 5kpc$.

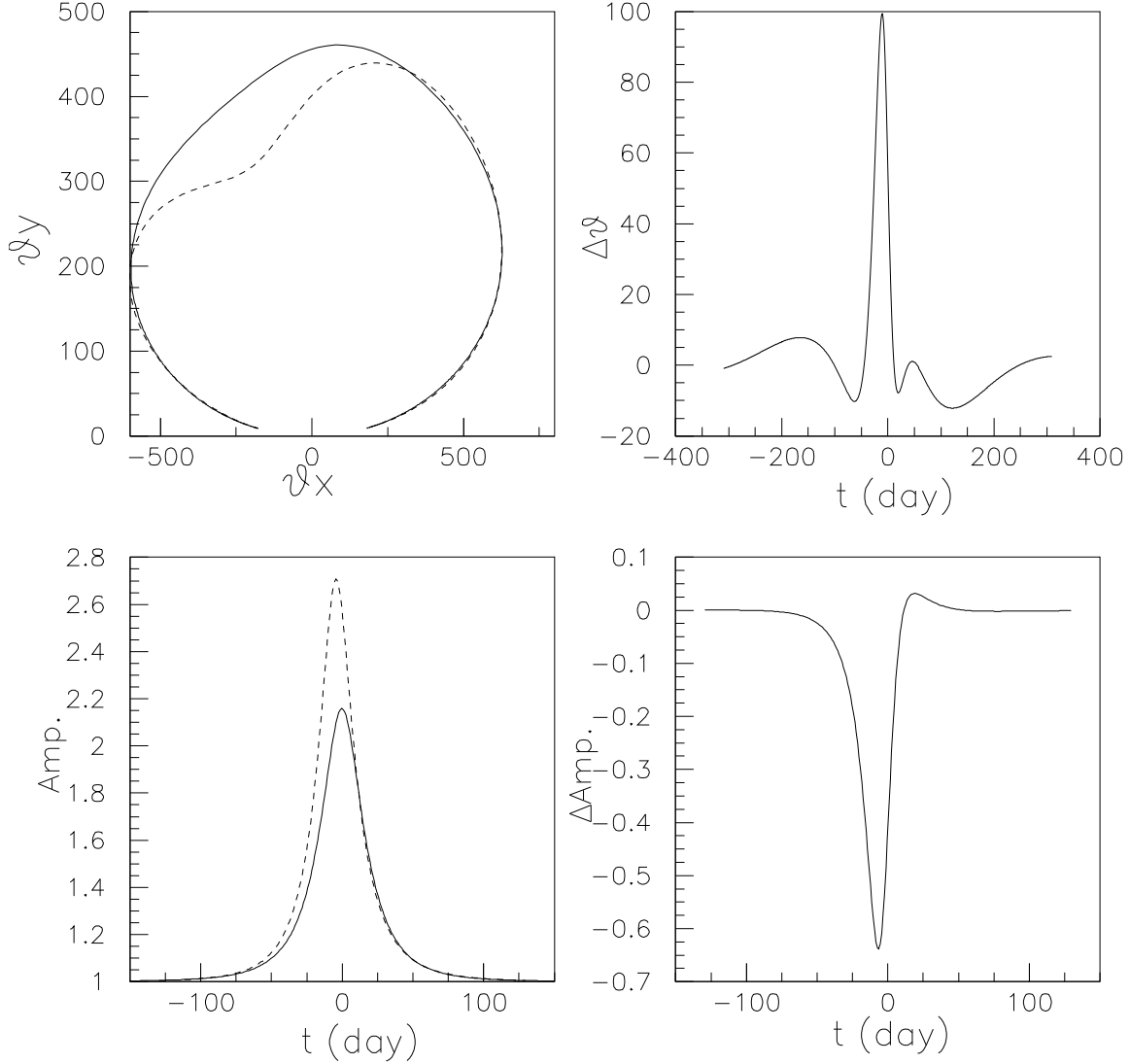


Fig. 2.— Astrometry and Photometry of a microlensing event in Kerr metric. The microlensing event for the static observer (solid-line) is compared with that of considering the parallax effect (dashed-line). Top-left panel shows the astrometry of center of images for both cases and top-right panel shows the contrast between them. The lower-left panel is the photometry and the lower-right panel is the contrast between them. The parameters of lens is chosen as $t_e = 40$ days, $t_0 = 0$ days, $u_0 = 0.5$, $M = M_\odot$, $D_{os} = 10kpc$ and $D_{ls} = 5kpc$ and spine is taken as $\mathbf{S} = (-\cos\frac{\pi}{3}\mathbf{i} + \sin\frac{\pi}{3}\mathbf{j}) \times 10^{41}Kgm^2s^{-1}$

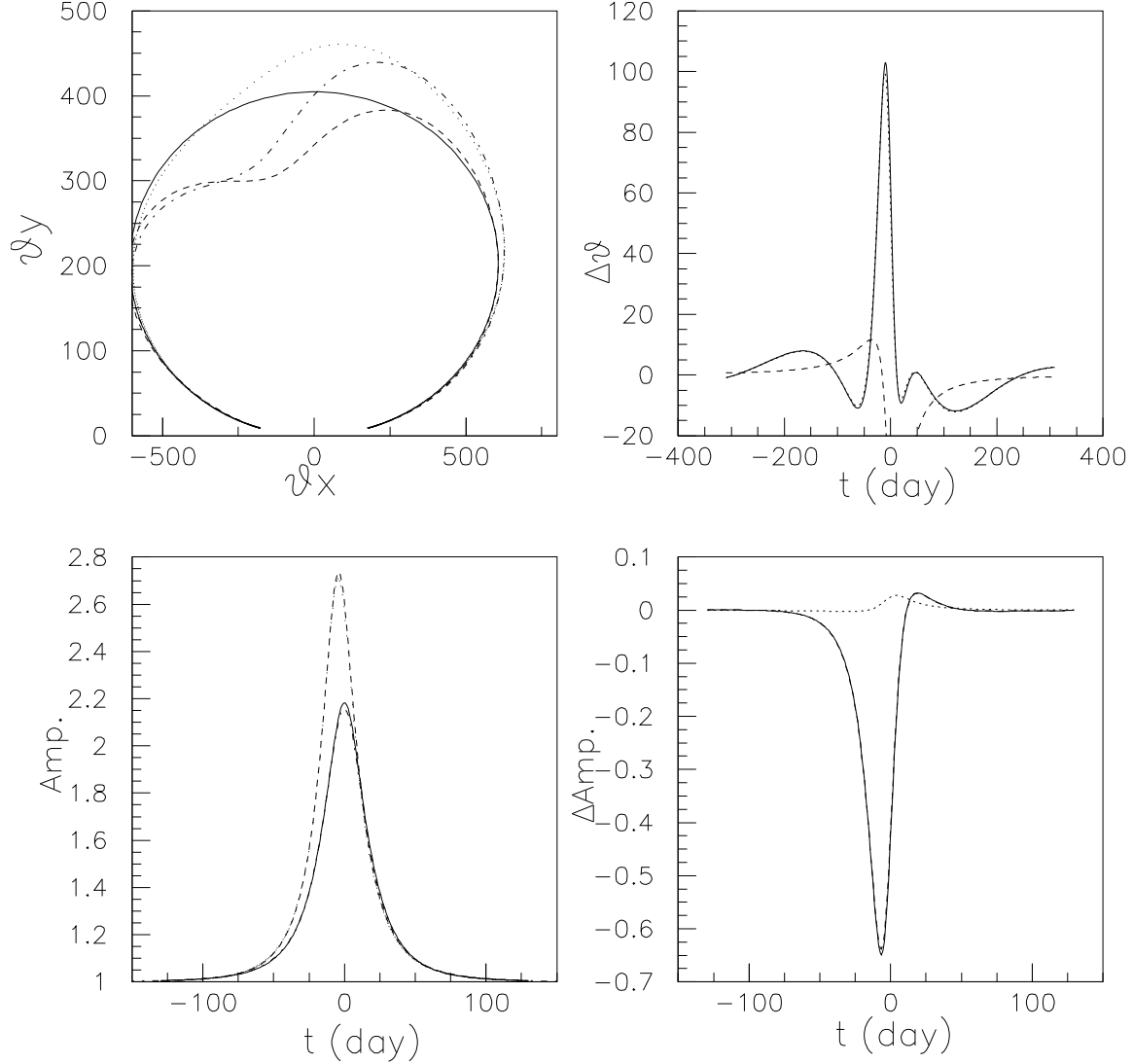


Fig. 3.— Comparison of the astrometry and photometry in the Schwarzschild and Kerr metrics. The parameters of lens are as in Figs. (1) and (2). At the top-left hand side panel, astrometry for the static observer in the Schwarzschild metric (solid-line), considering the parallax effect (dashed-line), in Kerr metric with static observer (dotted-line) and with the parallax effect (dashed-dotted line) is presented. The top-right panel shows the difference between the position of center of images for Schwarzschild and Schwarzschild-parallax (solid-line), Kerr and Kerr-Parallax (dotted-line) which in coincide to the fist curve and difference between the Kerr and Schwarzschild metrics (dashed-line). The lower plane is the photometry with an without parallax effects for Schwarzschild (Solid-line), with parallax (dashed-dotted line), Kerr (dashed-line) and Kerr with parallax (dotted line). At the right-down panel, the difference between the Schwarzschild and Schwarzschild-parallax (solid-line) and Kerr and Kerr-Parallax (dashed-line) which in coincide to the fist curve and difference between the Kerr and Schwarzschild metrics (dotted line).

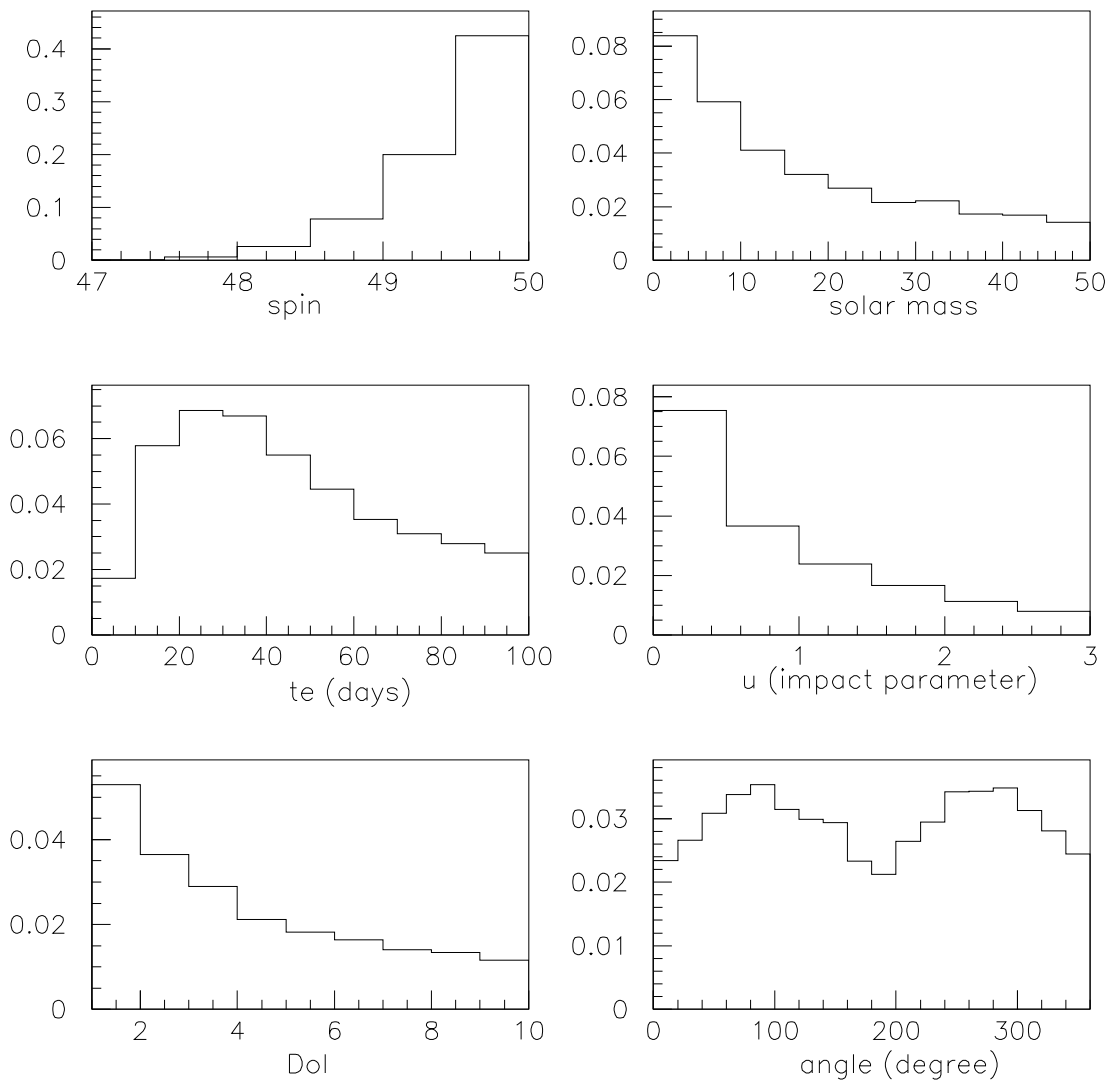


Fig. 4.— Fraction of lenses that can show the signature of spin for the telescope with $10\mu as$ angular resolution. The parameters of the lens, the spin, mass, Einstein crossing time, impact parameter, observer-lens distance and the orientation of spin with respect to the observer-lens-source plane are generated uniformly to show the sensibility of them to the rotating star detection.